

A new synchronization mechanism via Turing-like microscopic structures for CO oxidation on Pt(110)

R. Salazar and A.P.J. Jansen

*Schuit Institute of Catalysis (ST/SKA), Eindhoven University of Technology,
P.O. Box 513, 5600 MB Eindhoven, The Netherlands.*

V.N. Kuzovkov

Institute for Solid State Physics, University of Latvia, Kengaraga 8, LV-1063, Riga, Latvia.

(Dated: November 20, 2018)

We discuss an alternative to the traditional gas-phase coupling approach in order to explain synchronized global oscillations in CO oxidation on Pt(110). We use a minimalist microscopic model which includes structural Pt surface reconstruction via front propagation, and large diffusion rates for CO. The synchronization mechanism is associated with the formation of a Turing-like structure of the substrate. By using large parallel microscopic simulations we derive a scaling laws which allow us to extrapolate to realistic diffusion rates, pattern size, and oscillation periods.

PACS numbers: 82.65.+r; 82.20.Wt; 02.70.Tt; 82.40.Np; 89.75.Da

Oscillations appear in experiments of CO oxidation on Pt(110) in a very narrow parameter interval [1]. Additionally, it is also possible to observe pattern formation; about $T \sim 500\text{K}$ a crossover exist from spirals and fronts at low T to standing waves and chemical turbulence at high T . Experiments using fast scanning tunneling microscopy and field ion microscopy have clearly shown that fast kinetic processes are typically accompanied by the appearance of microscopic structures [2, 3, 4].

Although the diffusion of CO is fast, it does not provide a synchronization mechanism for the global oscillations, it is thought that the mechanism for global synchronization is coupling via the gas-phase [5]. This mechanism has been used widely in classical reaction-diffusion (RD) models. However, experiments have shown that particle dynamics on surfaces can be highly correlated [2], something which is not taken into account in RD models. This leads to differences between RD and experiments which can only be removed by including phenomenological corrections. An alternative mechanism for global synchronization of oscillation has been suggested based on spontaneous phase nucleation [6, 7]. This nucleation results in a random creation of dynamic defects and leads to global synchronization via stochastic resonance.

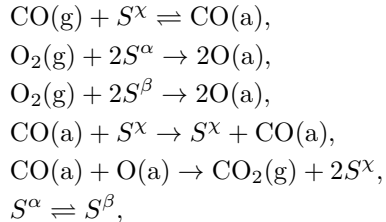
We present in this paper Monte Carlo (MC) simulations of a microscopic model for CO oxidation on Pt(110). We show that our model can produce global oscillations via a new mechanism showing microscopic structures without gas-phase coupling, coupling via stochastic resonance, or lateral interactions. The microscopic structures appear in the substrate, but they also support pattern formation in the adlayer on a mesoscopic length scale. In addition we provide a connection between these MC simulations and experimental results, via scaling laws.

MC simulations provide a systematic approach to include microscopic effects [8]. MC simulates directly the chemical reaction steps in a model, without averaging out particle correlations. Simulations of our model were performed by using a Cellular Automaton (CA) which has

been shown to be equivalent to MC [9]. A limitation of MC simulations has been the inability to deal with experimental system sizes and realistic diffusion coefficients. However, by using large parallel simulations as described in [10] we can now estimate results for experimental conditions. Using this parallel code we are able to simulate system sizes of about $1\text{ }\mu\text{m}$ with diffusion coefficients of about $10^{-10}\text{cm}^2\text{sec}^{-1}$. This approaches experimental conditions closer than any other previous MC simulation. Experimental values are for system sizes $10^2\text{ }\mu\text{m}$ or more and diffusion coefficient $10^{-6}\text{cm}^2\text{sec}^{-1}$. There is a gap between experimental and simulated rate constants, but, as we can vary the system size and the diffusion rate over a large range, we can derive scaling laws, which we can use to extrapolate the behavior predicted by our model to realistic system sizes and diffusion rates.

Our model has already been used in several studies [6, 11, 12]. O_2 adsorbs dissociatively onto two nearest neighbor sites with rate constant $(1-y)s_\chi$ with $\chi = \alpha, \beta$, where α denotes the 1×2 phase and β denotes the unreconstructed 1×1 phase of Pt(110) [1]. The experimental value for the ratio of the sticking coefficients of O_2 on the two phases is $s_\alpha : s_\beta \approx 0.5 : 1$. CO is able to adsorb onto a free surface site with rate constant y and it desorbs from the surface with rate constant k . Both reactions are independent of the surface phase to which the site belongs. In addition CO is able to diffuse via hopping onto a vacant nearest neighbor site with rate constant D . The $\text{CO} + \text{O} \rightarrow \text{CO}_2$ reaction occurs with rate constant R , when CO and O are nearest neighbors sites. CO_2 desorbs immediately forming two vacant sites. The $\alpha \rightleftharpoons \beta$ surface phase transition is modeled as a front propagation with rate constant V . For two nearest neighbor surface sites in the state $\alpha\beta$ the transition $\alpha\beta \rightarrow \alpha\alpha$ ($\alpha\beta \rightarrow \beta\beta$) occurs if none (at least one) of these two sites is occupied by CO. Summarizing the above transition definitions written in

the more usual form of reaction equations gives:



where S stands for a vacant adsorption site, χ stands for either α or β , and (a) and (g) for a particle adsorbed on the surface or in the gas phase, respectively. For additional details see Ref. [13]. Our simulations use special normalization of the rates: the adsorption rate for CO is related to the partial pressures by

$$y = \frac{P_{\text{CO}}}{P_{\text{CO}} + P_{\text{O}_2}}. \quad (1)$$

Comparing our rate constants with typical experimental values used in RD models [14, 15] we can estimate the unit of time in our simulation to be about $t_0 \approx 10^{-2}\text{s}$. All our rate constants are expressed in that unit of time. Lengths are expressed in units of the unit cell parameter a . The diffusion rate D is related to the experimental diffusion coefficient D_A by $D_A = a^2 D / z t_0$, where $z = 4$ is the coordination number.

The quality of the oscillations as a function of y has a typical resonance form. Well-defined oscillations are found near $y = 0.494$. Under certain condition, which we discuss below, these oscillations are global. Moving away from $y = 0.494$ we see first that the synchronization decreases and then a disappearance of the oscillations. We restrict ourselves to $y = 0.494$ (for a fixed values $k = 0.1$ and $V = 1$) in our simulations.

We have found that two situations are possible depending the system size, the diffusion rate, and on the initial conditions (IC). If the system is small or the diffusion is fast we find global oscillations. If the diffusion is too slow for a given system size the IC become important. We can again have global oscillations or the formation of patterns in the form of moving fronts and spirals.

To illustrate the synchronization mechanism Fig. 1 shows global oscillations. When the system is covered almost fully by CO the β islands in the α background grow (snapshots 1 and 2). When the size of the β islands is large enough the rate of adsorption of O_2 becomes larger than the adsorption of CO on the β zones (snapshots 3 and 4). At the same time the CO in the α zones is converted to CO_2 near to the borders with the β zones (snapshot 4). When the total coverage of oxygen becomes larger than CO, then the direction of the island growth is reversed (snapshots 4, 5, and 6) and α islands grow in the β background. When the size of the β zones is not large enough to keep the oxygen coverage larger than the CO coverage (snapshot 7), then both phases become covered by CO, and the cycle starts again (snapshot 8). The key point in this cycle is the existence of a critical size

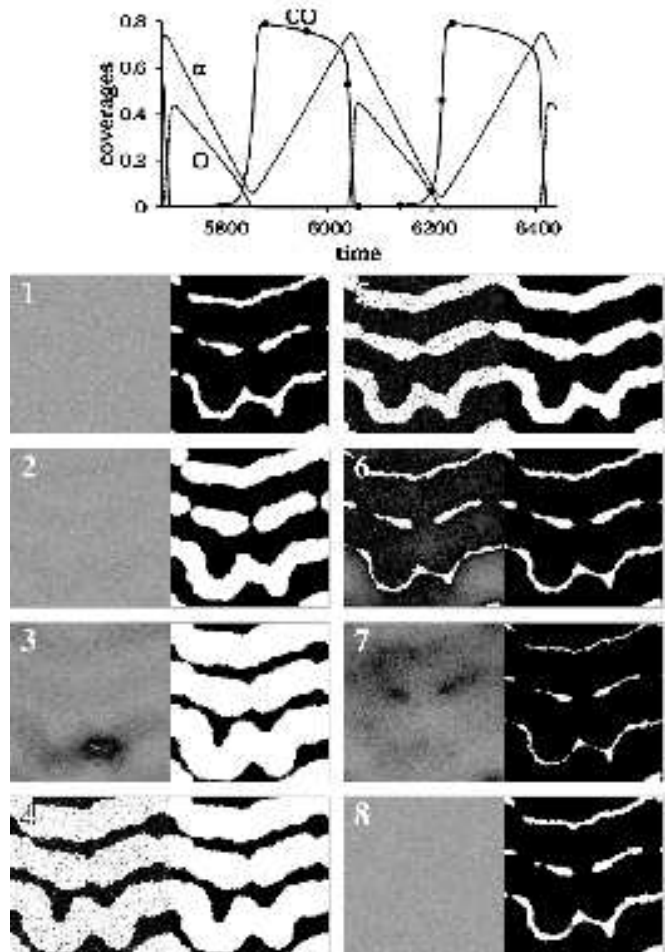


FIG. 1: Oscillations for $D = 4000$ and $L = 1024$ on the coverage CO (solid), oxygen (dashed), and α (dotted). Sequence of temporal snapshots correspond to the points in the upper figure. Each snapshot has two parts: In the left part we plot the chemical species; CO particles are grey and O particles are white, and empty sites are black. The right part shows the structure of the surface; α phase sites are black, and β phase sites are white.

of the β islands where oxygen becomes more stable than CO and a critical size of α islands where CO is more stable than oxygen. This corresponds to a phase transition produced by a varying size of these islands. This phase transition is driven by diffusion and the critical size of the islands depends on the diffusion rate as \sqrt{D} .

We found that the most important feature of the structures of the substrate is the typical distance between the islands; i.e., the correlation length l_c of these structures. For l_c we use the distance to the first maximum in the radially averaged correlation function of the substrate. The shape of the islands self-organizes through successive oscillations so that they cover the whole system with same sized islands separated by similar distances and small differences in size are removed. We note that our simple model of surface reconstruction by border propaga-

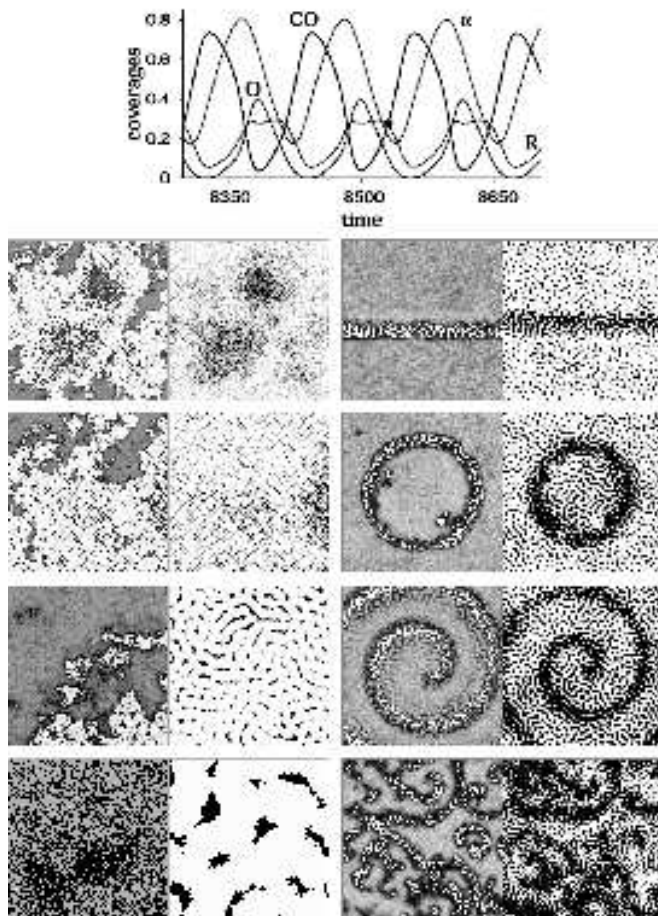


FIG. 2: Global oscillations and pattern formation with $D = 250$. Sections of the upper-left corner with $L = 8192, 4096, 1024$, and 256 are shown on the left side. The sections correspond to the dot in the temporal plot at the top. It shows the same information as Fig. 1, but it also includes the rate of CO_2 formation R . On the right side we have a wave front, a target, a spiral, and turbulence ($L = 2048$), which can be obtained with different initial conditions.

tion dynamic is sufficient to produce this effect. It yields synchronization at large scales even with relatively small diffusion rates. In Fig. 1 the diffusion length $\xi = \sqrt{DT}$, with T the period of the oscillations, is larger than the system size L . The synchronization is therefore trivial. In Fig. 2, however, a simulation is shown where the diffusion length is much smaller than the lattice size, but larger than the correlation length. So the diffusion synchronizes the oscillations on neighboring islands, and the self-organization leads to global oscillations.

In cases where the synchronization is even better, as with large D values, islands tend to be grouped forming rolls which are parallel (see Fig. 1). The structures formed in this way resemble labyrinthic Turing structures. Moreover a percolating connection between islands can be observed. The full analytical analysis of this behavior is far from trivial, however the difference of the mobility for CO and O, could be sufficient for get a Tur-

ing instability in this model.

When the diffusion is slow pattern formation can also occur as on the right of Fig. 2. The distance between the centers of α and β islands is the same as for the global oscillations, but the size of the islands differ for different parts of the system. These differences will not be removed as in the fully synchronized cases. As a consequence a delay or detuning will appear in the oscillations for different parts of the surface, which can create fronts, target pattern patterns, spirals, and turbulence. A cross-section of one of these fronts shows a delay between the pulse of the adsorbates and the pulse of the substrate phases, which determines the direction of propagation. This is a common feature of excitable, bistable systems, such as the activator-inhibitor models. The most remarkable feature is that these fronts appear on top of fixed Turing-like structures which are present even in these incompletely synchronized cases. So we have within our model two different length scales for pattern formation; excitable dynamics for fronts and spirals on a mesoscopic scale (Hopf instability, [14]), and quasi-fixed Turing-like microscopic structure.

A scaling analysis for the Turing structures and the oscillations for the fully synchronized case is presented in Fig. 3. We show the scaling behavior for the period of oscillations T and the correlation length l_c as a function of diffusion rate D . Numerically we found that the relations $T(D) \sim D^\nu$ and $l_c(D) \sim D^\mu$ holds with $\nu = 0.4849 \pm 0.016$ and $\mu = 0.5069 \pm 0.01$. For large D values a large system size is required to compute $l_c(D)$ precisely. For instance for $D = 8000$ we use $L = 8192$. Additionally large diffusion rates means that most of the time is spend moving particles; on 8000 diffusion steps only one chemical reaction happens. Also the simulation time increase because the oscillation period increases with D .

A relationship $T(D) \sim l_c(D) \sim D^{1/2}$ seems quite reasonable, as our model has fast diffusion. In fact the scaling law for l_c is the consequence of scaling law for T . The width of the Turing structure oscillates on a length of order l_c due to the phase propagation with rate V . The period is related to these by $l_c \sim VT$. If the velocity V is constant, then $l_c \sim T$. Fig. 3 was computed for a fixed value of V . Using a larger value for the velocity parameter we can obtain larger correlation lengths l_c and smaller periods T , but the scaling remains the same. We have found for the Turing-synchronized oscillations that the relation $T \sim V^{-1/2}$ also applies as in [6, 7, 13]. So we have an important scaling law in form $T = c\sqrt{D/V}$, where $c \sim 10$. An estimate for the oscillation period for realistic diffusion rates $D_A \sim 10^{-6} \text{ cm}^2 \text{ sec}^{-1}$ we have $D \sim 10^8$. The experimental oscillations period is $\tau = t_0 T$ with $t_0 \sim 10^{-2} \text{ sec}$ and $\tau = 10 \text{ sec}$. The value V predicted by our model for that value of τ is then of the order of $V \sim 10^2$.

We propose that the minimal condition to have global oscillations is that the diffusion length ξ is at least of the order of the correlation length l_c : $\xi = l_c$ ($\xi = \sqrt{DT}$ and

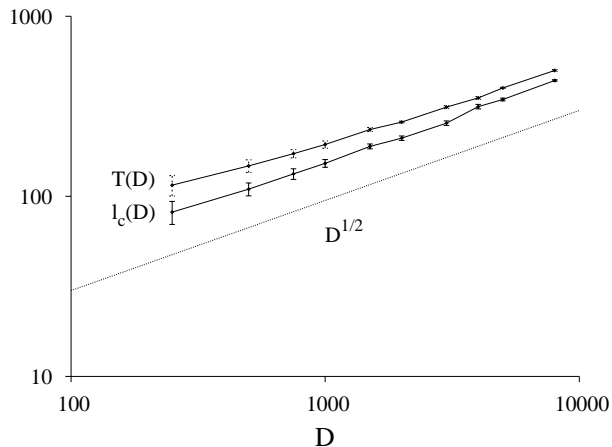


FIG. 3: Scaling behavior for the period of oscillations $T(D)$ and the correlation length $l_c(D)$ (units).

$l_c = VT$, $c \sim 10$). Critical values for the diffusion rate and the correlation length are then

$$\begin{aligned} D &= c^2 V^3 \\ l_c &= c^2 V^2. \end{aligned} \quad (2)$$

For $V = 1$ we get the order of the parameters used in Fig. 2 (left side), $D \sim 10^2$ and $l_c \sim 10^2$ where global oscillations are possible but infrequently.

Diffusion is a thermally activated process so we can compare our proposal, Eqs. (2), with the experimental crossover at $T \sim 500$; for lower temperatures where fronts and spirals appear, we have lower diffusion rates, $\xi <$

l_c and the synchronization mechanism is not stable and produces patterns similar to on the right of Fig. 2. On the other hand for large temperatures where standing waves and chemical turbulence appear, we have large diffusion rates, $\xi > l_c$, and we get better synchronization, as in Fig. 1. For $\xi = l_c$ we get the crossover, Eqs. (2) holds and we get the minimum criteria for synchronization, as in Fig. 2 on the left.

Using $V = 10^2$ in Eqs. (2) we get for the critical value of diffusion rate $D \sim 10^8$, which corresponds to the experimental value of $D_A \sim 10^{-6} \text{cm}^2 \text{sec}^{-1}$. This confirms our crossover idea. For correlation length $l_c \sim 10^6$ (in units of cell parameter a) we have a size $\sim 10^2 \mu\text{m}$ which is of the order of magnitude of the standing waves observed in experiments [15]. Near crossover it is possible to interpret V also as the velocity v of the fronts and spirals. For $V = 10^2$ we have $v = aV/t_0 \sim 10^{-4} \text{cm s}^{-1}$, in agreements with experiments [16].

To summarize we present in this paper a new mechanism for synchronization of global oscillations based on microscopic Turing-like structures in the reconstruction of the surface. In cases with incomplete synchronized oscillations the adlayer has a mesoscopic second characteristic length. This is the first actual demonstration of a double length scale. Scaling laws are analyzed to connect the model to experimental parameter values.

This work was supported by the Nederlandse Organisatie voor Wetenschappelijk Onderzoek (NWO), and the EC Excellence Center of Advanced Material Research and Technology (contract N 1CA1-CT-2080-7007). We would like to thank the National Research School Combination Catalysis (NRSCC) for computational facilities.

-
- [1] R. Imbihl, G. Ertl, *Chem. Rev.* **95**, 697 (1995).
 - [2] J. Winterlin, *Chaos*, **12**, 108 (2002).
 - [3] S. Völkening, K. Bedürftig, K. Jacobi, J. Winterlin, G. Ertl, *Phys. Rev. Lett.* **83**, 2672 (1999).
 - [4] J. Winterlin, S. Völkening, T.V.W. Janssens, T. Zambelli, G. Ertl, *Science* **278**, 1931 (1997).
 - [5] H. Levine, X. Zou, *Phys. Rev. Lett.* **69**, 204 (1992).
 - [6] O. Kortlüke, V.N. Kuzovkov, W. von Niessen, *Phys. Rev. Lett.* **83**, 3089 (1999).
 - [7] O. Kortlüke, V.N. Kuzovkov, W. von Niessen, *Phys. Rev. E* **66**, 036139 (2002).
 - [8] J.J. Lukkien, J.P.L. Segers, P.A.J. Hilbers, R.J. Gelten, A.P.J. Jansen, *Phys. Rev. E* **58**, 2598 (1998).
 - [9] O. Kortlüke, *J. Phys. A* **31**, 9185 (1998).
 - [10] R. Salazar, A.P.J. Jansen, V.N. Kuzovkov, nlin.CG/0207059.
 - [11] O. Kortlüke, V.N. Kuzovkov, W. von Niessen, *Phys. Rev. Lett.* **81**, 2164 (1998).
 - [12] V.N. Kuzovkov, O. Kortlüke, W. von Niessen, *Phys. Rev. Lett.* **83**, 1636 (1999).
 - [13] O. Kortlüke, V.N. Kuzovkov, W. von Niessen, *J. Chem. Phys.* **110**, 11523 (1999).
 - [14] M. Bär, M. Hildebrand, M. Eiswirth, M. Falcke, H. Engel, M. Neufeld, *Chaos* **4**, 499 (1994).
 - [15] A. von Oertzen, H.H. Rotermund, A.S. Mikhailov, G. Ertl, *J. Phys. Chem. B* **104**, 3155 (2000).
 - [16] M. Falke, M. Bär, H. Engel, M. Eiswirth, *J. Chem. Phys.* **97**, 4555 (1992).